

Ultrasensitive laser measurements without tears

Philip C. D. Hobbs

Several easily implemented devices for doing ultrasensitive optical measurements with noisy lasers are presented. They are all-electronic noise cancellation circuits that largely eliminate excess laser intensity noise as a source of measurement error and are widely applicable. Shot-noise-limited optical measurements can now easily be made at baseband with noisy lasers. These circuits are especially useful in situations where strong intermodulation effects exist, such as current-tuned diode laser spectroscopy. These inexpensive devices (parts cost \approx \$10) can be optimized for particular applications such as wideband or differential measurements. Although they cannot eliminate phase noise effects, they can reduce amplitude noise by 55–70 dB or more, even in unattended operation, and usually achieve the shot-noise limit. With 1-Hz signal-to-noise ratios of 150–160 dB, they allow performance equal or superior to a complex heterodyne system in many cases, while using much simpler dual-beam or homodyne approaches. Although these devices are related to earlier differential and ratiometric techniques, their noise cancellation performance is much better. They work well at modulation frequencies from dc to several megahertz and should be extensible to \approx 100 MHz. The circuits work by subtracting photocurrents directly, with feedback applied outside the signal path to continuously adjust the subtraction for perfect balance; thus the excess noise and spurious modulation ideally cancel at all frequencies, leaving only the shot noise. The noise cancellation bandwidth is independent of the feedback bandwidth; it depends only on the speeds of the photodiodes and of the bipolar junction transistors used. Two noise-canceled outputs are available; one is a high-pass filtered voltage proportional to the signal photocurrent and the other is a low-pass filtered voltage related to the log ratio of the signal and comparison photocurrents. For reasonable current densities, the noise floors of the outputs depend only on the shot noise of the signal beam. Four variations on the basic circuit are presented: low noise floor, high cancellation, differential high power, and ratio-only. Emphasis is placed on the detailed operation and design considerations, especially performance extension by compensation of the nonideal character of system components. Experience has shown that some applications advice is required by most users, so that is provided as well. © 1997 Optical Society of America

1. Introduction

Excess noise, spurious modulation, and power drift in lasers are common problems in optical measurements. The noise and spurious signals are usually worst at low modulation frequencies and can easily reach 50 dB above shot noise—even quite far from dc—which makes ultrasensitive optical measurements difficult. A great deal of work has been done on this problem, both to make lasers quieter and to circumvent the worst effects of the remaining noise.

Most precise optical measurement systems apply some sort of modulation to the beam to make their output signals periodic in time at a frequency as far from the low-frequency noise as necessary; these are

then detected in bandwidths sufficiently narrow to exclude most of the excess noise. Typical examples are heterodyne interferometers,¹ frequency modulation methods,^{2,3} beam-chopping systems with lock-in detection,⁴ and fast-scanning systems with signal averaging. (In this paper, excess noise refers both to true noise above the shot-noise level and to spurious modulation of the beam intensity, due, for example, to baseband mode beats or power supply ripple.)

Optical feedback stabilization of several kinds^{5,6} and all-electronic noise rejection schemes such as differential detection^{7–10} (subtraction) and normalization by analog division¹¹ are used extensively; but when used unaided, they are limited by their noise floors, bandwidths, or finicky adjustment requirements to relatively low-performance applications. Of all the techniques listed, none results in measurements at the shot-noise limit except heterodyne interferometry.

Chopping techniques are too slow to escape the excess noise region, although as they move the mea-

The author is with the IBM Thomas J. Watson Research Center, P.O. Box 218, Yorktown Heights, New York 10598.

Received 30 April 1996.

0003-6935/97/040903-18\$10.00/0

© 1997 Optical Society of America

surement bandwidth a little away from dc, they may sometimes help considerably; signal-averaging systems are usually somewhat better in this regard. Frequency modulation methods can escape the excess noise region without needing an interferometer, but because the actual measurement is taken on one weak optical sideband, most of the laser power is wasted, and the signal-to-noise ratio (SNR) of the measurement is considerably worse than the signal-to-shot-noise ratio of the entire beam. Heterodyne interferometers allow measurements to be made at frequencies far from the baseband noise, often allowing the shot-noise limit to be reached; however, in addition to the expense and complexity involved, a heterodyne measurement with the same temporal response as a homodyne or other baseband technique has twice the noise bandwidth (and so is 3 dB noisier for the same noise power spectral density) because optical frequencies above and below the carrier must be accepted. An alternative technique is all-electronic noise cancellation,¹²⁻¹⁴ which allows shot-noise-limited optical measurements at baseband with noisy lasers. By relying on the near-ideal properties of photodiodes, bipolar junction transistors (BJT's), and most optical systems, it is able to suppress excess laser noise by as much as 60 dB from dc to tens of megahertz. The system uses a BJT differential pair to split the current from a reference photodiode (which is fed a sample of the beam) in a subtractive circuit, with negative feedback providing continuous adjustment of the balance. In addition to high levels of excess noise suppression, the devices exhibit noise floors limited only by the shot noise of the signal beam. This circuit has been used to perform ultrasensitive laser absorption spectroscopy,^{15,16} coherent lidar,¹⁷ and other measurements with better performance and simpler apparatus than hitherto possible.

In this paper is presented design considerations, performance limitations, and several generalizations, including the important case of differential measurements. It concludes with detailed schematic diagrams and a discussion of the several versions, and a mathematical Appendix.

2. Laser Noise

Much of the work of designing an ultrasensitive optical apparatus involves circumventing the effects of laser noise. Laser noise arises in a great variety of ways, so an exhaustive list is difficult to give. A few of the more annoying types are baseband mode beats in gas lasers, mode hopping, instability caused by unintended optical feedback into the laser cavity, wiggle noise,¹⁸ and electrically or mechanically induced modulation from such sources as cooling water turbulence and power supply ripple.

Some laser applications, such as heating¹⁹ and pumping nonlinear elements or other lasers,²⁰ require the beam itself to be stable in amplitude because it is driving the system. Others, such as the highest-resolution spectroscopy, require low noise in both phase and amplitude because both contribute to the spectral width of the laser line (the frequency

modulation noise is generally far worse). In these cases, there is no alternative but to stabilize the laser as much as possible.

In most other measurements, photocurrent fluctuations resulting from laser amplitude noise are the primary nuisance. Both the signal photocurrent being measured and any static background that may be present are proportional to the laser power, and so intensity fluctuations translate directly into measurement noise. The laser-noise-induced fluctuations of the background appear as additive noise on top of the signal, while those of the signal itself appear as multiplicative noise, causing noise intermodulation, the impressing of noise sidebands on the desired signal.

In a measurement of a small shift on a large background, the fluctuations of the background are the worst problem, so experimenters usually aim to make zero background measurements, which minimize noise and drift from these fluctuations. In most such cases, the shot-noise contribution is not reduced by going to the zero background methods, so they would lose some of their attractiveness if truly quiet lasers were available. Exceptions to this rule include fluorescence, photochemical grating, and other dark-field measurements. These have other disadvantages, however, especially in their requirement for photomultiplier tubes, which have poor quantum efficiency and therefore lower SNR. Noise intermodulation is not addressed by zero background techniques, nor by most of the other available noise reduction methods.

A. Feedback Stabilization

Drift and low-frequency noise in lasers are often dealt with by using feedback stabilization techniques,⁶ by using external modulators or injection current modulation. These techniques work fairly well, but with the exception of current feedback with diode lasers, they tend to be complicated or expensive.

In measurements not involving squeezed light, the best-case noise floor of a photocurrent i is set by its shot-noise current, given by

$$i_n = \sqrt{2eiB}, \quad (1)$$

where e is the electron charge and B is the measurement bandwidth.

All the noise suppression methods that follow rely on a comparison of one or more signal beams to a comparison beam. (The term comparison beam is better than the common term reference beam and than my earlier term sample beam, because it avoids confusion in interferometric and spectroscopic applications.)

In any technique that stabilizes one noisy signal by reference to another, the uncorrelated parts of the noise (i.e., the shot-noise contributions) ideally obey

$$\frac{1}{\text{SNR}_{\text{out}}} = \frac{1}{\text{SNR}_{\text{signal}}} + \frac{1}{\text{SNR}_{\text{comp}}}, \quad (2)$$

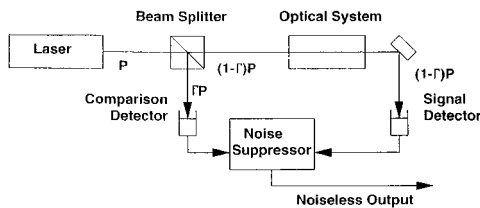


Fig. 1. Block diagram of a generic all-electronic laser noise suppression scheme. The beam itself is unmodified; the noise improvement comes from combining signal and comparison photocurrents.

where $\text{SNR}_{\text{signal}}$, SNR_{comp} , and SNR_{out} are, respectively, the power signal-to-noise ratios of the signal, comparison photocurrents, and combined photocurrents. The effects of finite bandwidth and technical noise in the combining circuitry are ignored. Their power noise-to-signal ratios add, at least for noise frequencies well within their bandwidths. Thus such methods can at best bring the SNR of the resulting beam (or photocurrent) to the signal-to-shot-noise ratio of the comparison beam; if the two photocurrents are equal, then the noise of the output is 3 dB above that of the signal beam alone.

In feedback stabilizers, $\text{SNR}_{\text{signal}}$ is the signal-to-shot-noise ratio of the output beam with the stabilizer loop opened, and SNR_{out} is that of the output beam with the stabilizer operating. Most users dislike losing half or more of their laser power in a stabilizer, so the comparison beam is usually chosen to be appreciably weaker than the main one; thus it contains relatively more shot noise, and this contributes to a high-noise floor.

Besides the noise floor problem, feedback stabilizers are intrinsically rather narrowband. For example, if 40-dB noise suppression is needed to reach the shot-noise floor, the feedback system must remove 99% of the noise current, so its closed-loop gain error must be less than 1%; assuming an open-loop unity gain bandwidth of 0.5 MHz and a 1-pole rolloff, this occurs at 5 kHz. Feedback stabilization is worthwhile for many kinds of optical systems but is incapable of reaching the shot-noise limit with noisy lasers.

B. All-Electronic Noise Suppression

All-electronic schemes have been known for some time as well⁷ and have been widely used. As can be seen from the block diagram in Fig. 1, these schemes differ from those discussed above in that no attempt is made to stabilize the laser beam itself, only the photocurrent at the output of the apparatus. The beam is sampled at the laser and detected to obtain a comparison photocurrent with the same fractional excess noise as that from the signal beam (which represents the output of the optical system). The two are then combined in some fashion to obtain an output current that, ideally, is completely free of excess noise.

Such methods rely on two important properties of most optical systems, namely, extremely wide tem-

poral bandwidth and the use of highly linear photodetectors, such as photoconductive-mode photodiodes. The wide bandwidth guarantees that (if path delays are small) the optical system will not apply any gain variation or phase shift to the modulation of the beam—the instantaneous, fractional, excess amplitude noise of the comparison beam will be identical with that of the signal beam—so that if the cancellation is done properly, the noise suppression should be essentially perfect. The linearity of the photodiodes allows excellent cancellation performance with unmatched diodes, even if they are running at appreciably different current densities. With such fortunate circumstances, all-electronic noise cancellation should be extremely effective.

In the past, two all-electronic methods have been common, namely subtraction^{1,21,22} and division.²³ In a subtractive noise rejection scheme, the comparison photocurrent is subtracted from the signal current. If the optical system is adjusted perfectly so that the two photocurrents are exactly equal, the excess noise and dc cancel, leaving only the signal and shot noise. Subtracters can have wide bandwidths, since the photocurrents can be subtracted directly (without prior conversion to voltages, which introduces poorly controlled phase shifts) and because the noise cancellation does not depend on feedback. The improvement is seldom more than 20 dB, because the adjustment required is finicky and because the intensity of the signal beam often varies somewhat during a measurement (e.g., from scanning), so that the currents cannot be exactly equal at all times. In addition, since the shot-noise currents of the signal and comparison photocurrents statistically are independent, they obey Eq. (2) and thus limit the system noise floor to 3 dB above the shot noise of the signal beam alone.

Dividers avoid the requirement for precise adjustment by dividing the signal current by the comparison current, hence canceling the fractional (rather than absolute) noise deviations. They have great attractions in theory, because dividing out the instantaneous intensity provides compensation for drift and noise intermodulation as well as removing additive excess noise. Dividers need not in principle suffer from the 3-dB additional noise problem of subtracters, since the comparison beam can be made stronger than the signal beam (and so relatively quieter). Unfortunately, dividers tend to be slow, so that the suppression bandwidth is limited and noisy, as suggested by the following example.

The Burr-Brown MPY-634 is neither the fastest nor the quietest divider available, but has a good compromise of noise, speed, and accuracy for this application. With a full-scale (10-V) denominator (the best case), it has a noise spectral density of approximately $1 \mu\text{V}/\sqrt{\text{Hz}}$ with a zero numerator and $2 \mu\text{V}/\sqrt{\text{Hz}}$ with a 10-V numerator; this is approximately 60 dB worse than the best operational amplifiers. Since its maximum input level is 10 V, its maximum SNR is 134 dB in a 1-Hz bandwidth. With appropriately chosen current-to-voltage con-

verter (transresistance amplifier) gain, and if the signal level is reduced by 3 dB to avoid clipping, this is equivalent to the signal-to-shot-noise ratio of a photocurrent of 8 μA . With a red helium neon laser and a silicon PIN diode (responsivity 0.3 A/W), that implies that a 27- μW laser beam can be quieted to 3 dB above the shot noise (granted a noiseless comparison beam), but a 3-mW beam, well within the linear operating regime of many photodiodes, can be quieted only to 20 dB above the shot noise, a poor performance.

Because of their use of feedback in the signal path and the frequency compensation problems alluded to above, dividers have poor high-frequency performance; swept sine measurements (0.2-V p-p. plus 7-V dc applied to both numerator and denominator, which were connected in parallel) on the unit mentioned above reveal 42-dB small-signal suppression at 100 Hz, deteriorating steadily above about 5 kHz, to 22 dB at 100 kHz, and virtually zero at 1 MHz.

Subtractors eliminate the additive excess noise, but can do nothing to suppress noise intermodulation; dividers in principle eliminate both. In high-accuracy (as opposed to merely high-dynamic-range) applications, where the signal is well above the additive noise floor and must be measured precisely, noise intermodulation limits the measurement accuracy to the SNR of the laser beam. For this reason, open-loop subtractors are most suitable for measurements of small changes in intensity with lasers that are already reasonably quiet.

For some purposes, then, dividers and open-loop subtractors can be very useful, but in general using them unaided does not allow shot-noise-limited measurements with noisy lasers.

3. Laser Noise Canceller

A. Principle

The open-loop subtractor can be improved substantially in many areas by the use of negative feedback outside the signal path, to continuously adjust the matching between the two photocurrents. By applying this idea, simple systems can be made that achieve the shot-noise limit without adjustments with most lasers; these systems are the subject of the remainder of this paper.

Feedback control requires an electronically variable current splitter that does not degrade the strict proportionality between the signal and comparison photocurrents and an electronic criterion for when the circuit is in balance. Figure 2 shows such a splitter. The comparison beam is made somewhat stronger than the signal beam, and the comparison photocurrent is split between two paths by using a bipolar transistor pair Q_1/Q_2 . The ratio of the collector currents of Q_1 and Q_2 is controlled by the difference $\Delta V_{BE} = V_{BE2} - V_{BE1}$ in their base emitter voltages. In the Ebers-Moll model

$$\frac{i_{C2}}{i_{C1}} = \exp\left(\frac{e\Delta V_{BE}}{kT}\right). \quad (3)$$

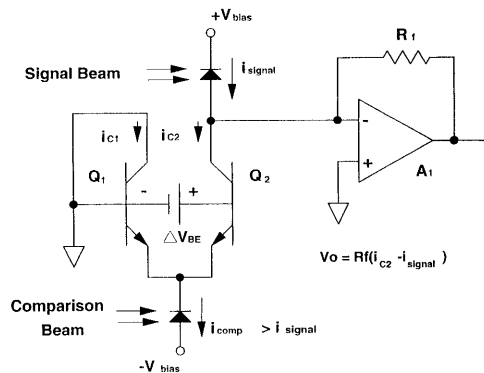


Fig. 2. Simplified schematic diagram showing the use of a BJT differential pair as a variable current splitter. The splitting ratio depends on ΔV_{BE} but not on i_{comp} , so the fluctuations split just the same way as the dc.

The BJT is unique in that this ratio does not depend on the value of i_{comp} ; its transconductance g_m ($g_m = \partial i_C / \partial V_{BE}$) is proportional to its collector current, which makes BJT differential pairs highly linear as current splitters. Thus fluctuations in i_{comp} split in exactly the same ratio as the dc, so the differential pair will not degrade the noise cancellation, within the limits set by the BJT gain bandwidth product f_T . Devices with good log conformity exhibit constant splitting ratios over several decades of collector current. To use this circuit, we make sure i_{comp} is somewhat larger than i_{signal} and adjust ΔV_{BE} to dump the extra to ground by way of Q_1 . Used alone, this adjustment would still be finicky and manual, but it provides the electronic control needed.

The balance criterion is simple; since the excess noise splits just as the dc, ideal noise cancellation occurs when the total dc photocurrent into the summing junction of transresistance amplifier A_1 is zero.

The combination of these two ideas yields the basic noise canceler, shown in Fig. 3, which uses negative feedback to keep the splitting ratio adjusted exactly. This circuit combines simplicity, freedom from adjustments, and good performance. Besides the differential pair Q_1-Q_2 and transresistance amplifier A_1 , there is an integrating servo amplifier A_2 that adjusts ΔV_{BE} to force the dc output of A_1 (and hence the dc current into A_1 's summing junction) to be zero, thus ensuring proper balance. Cascode transistor Q_3 prevents the capacitance of the signal photodiode from loading the summing junction, which may allow as much as 40 times improvement in the amplifier bandwidth compared with a straightforward transresistance amplifier with the same feedback resistance. A small capacitor in parallel with R_f may help in controlling any high-frequency gain peaking in A_1 .

The feedback loop can be as fast or as slow as desired because the bandwidth of effective cancellation does not depend on the feedback bandwidth f_c , only on the f_T of the transistors; the loop just tinkers with the adjustment. Because feedback is keeping the average voltage at the A_1 's output zero, A_1 's out-

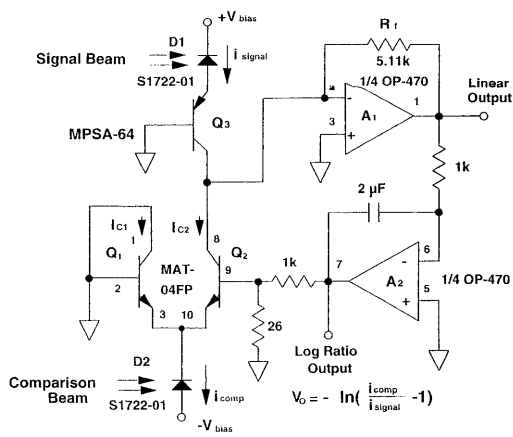


Fig. 3. Schematic diagram of the basic noise canceller. The BJT current divider Q_1/Q_2 is controlled by servo amplifier A_2 so that the dc output of transresistance amplifier A_1 is zero. This ensures that i_{signal} and i_{C2} are equal. Because the fluctuations are proportional to the dc, the excess noise cancels identically at all frequencies of interest, independently of the feedback bandwidth.

put is a high-pass filtered version of the signal photocurrent, minus the excess noise; its corner frequency is f_c .

Since the instantaneous excess noise fluctuations of the photocurrent are exactly proportional to their dc level, as discussed above, application of negative feedback to one of the transistor bases to keep the net dc photocurrent at zero results in essentially perfect noise cancellation out to very high frequencies, regardless of the bandwidth of the feedback loop. As an added benefit, the feedback voltage offers an alternative output; ΔV_{BE} is related to the ratio of the comparison current to the signal current (within the feedback bandwidth) by Eq. (3),

$$\Delta V_{BE} = -\frac{kT}{e} \ln\left(\frac{i_{\text{comp}}}{i_{\text{signal}}} - 1\right). \quad (4)$$

It is shown in Appendix A that if the emitter current of a differential pair has full shot noise, both collector currents have exactly full shot noise also, independent of the splitting ratio; thus the expected noise level of the output of A_1 is 3 dB above the shot noise of the signal current alone:

$$V_{NA1} = R_1 \sqrt{4eBi_{\text{signal}}}, \quad (5)$$

where B is the bandwidth and R_1 is the feedback resistor of A_1 . If the comparison beam contains signal information, as in a differential measurement, the SNR of the measurement can achieve the shot-noise level, but otherwise it is limited to 3 dB worse.

The noise at the output of A_2 is obtained by multiplying the total shot-noise current by the partial de-

rivative of V_{A2} with respect to i_{signal} :

$$\begin{aligned} V_{NA2} &= \frac{1}{\gamma} \frac{kT}{e} \sqrt{4e} \frac{1}{i_{\text{signal}}} \left(\frac{1}{1 - \frac{i_{\text{signal}}}{i_{\text{comp}}}} \right), \\ &= \frac{2kT}{\gamma \sqrt{e} i_{\text{signal}}} \left[1 + \exp\left(\frac{e\gamma V_{A2}}{kT}\right) \right], \end{aligned} \quad (6)$$

where γ is the voltage divider gain (0.025 here).

The voltage divider on the base of Q_2 performs three functions: It reduces the swing of A_2 so that the base-collector junction cannot be Zenered or forward biased enough to cause servo lockup. The choice of a 40:1 division ratio approximately cancels the factor of kT/e from Eq. (4), resulting in a scale factor of 2 V near null rather than 50 mV (1% change in $i_{\text{signal}}/i_{\text{comp}}$ gives a 20-mV change at A_2). It also reduces the contribution of the input voltage noise of A_2 to the total circuit noise. Most opamps have at least several nanovolts per root hertz noise, which is considerably worse than the 1-nV/ $\sqrt{\text{Hz}}$ noise of good transistors; this will degrade the noise floor of the final circuit if the voltage divider is not used. The Thévenin resistance of the divider should be kept small.

If the feedback signal is used as the output, the performance is much like that of a divider in that intermodulation between noise and signal is suppressed (since ΔV_{BE} depends only on the ratio of the two photocurrents). One important difference is that the new system does not get noisier as its loop bandwidth is approached, as dividers do; because the dc cancellation guarantees the cancellation of additive noise at all frequencies of interest, only the suppression of noise intermodulation declines. Another way of looking at this is that A_2 is integrating a signal (A_1 's output) whose noise has been canceled at all frequencies, so the additive noise cancellation bandwidth of the log output is independent of the feedback bandwidth. This is a remarkable fact, because it means that the entire bandwidth of the log ratio output is useful for highly sensitive measurements rather than only 1% or so as with dividers and feedback systems. The cancellation of noise intermodulation does depend on the feedback bandwidth.

The log output is especially useful for situations in which the noise intermodulation is strong, such as current-tuned diode laser spectroscopy^{15,16}; there the laser power may vary by as much as 2 or 3 to 1 during a scan, making small absorption peaks inconspicuous on a huge sloping background if this circuit (or some other background reduction technique) is not used. For applications such as this, Q_1 and Q_2 should be a monolithically matched pair to ensure that their temperatures are the same and that the dc offset voltage error in V_{A2} is small; if the log output is not needed, Q_1 and Q_2 may be replaced by discrete devices such as 2N3904's, which cost only a few cents.

There is nothing in the system that forces the feedback loop to be slow. The loop bandwidth f_c is found

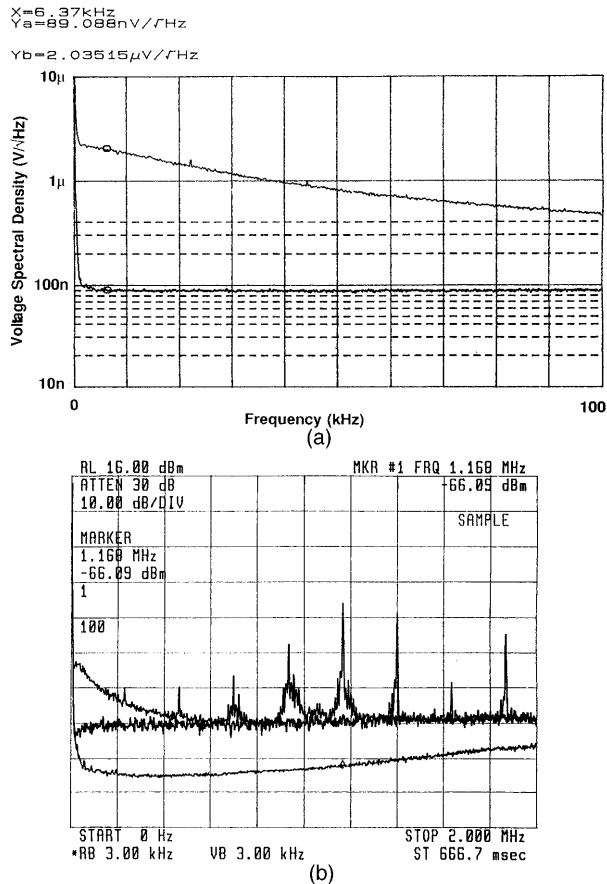


Fig. 4. Performance of the basic noise canceler of Fig. 3 with a 40-mW, 532-nm diode-pumped Nd:YAG laser exhibiting significant low-frequency noise and several peaks in the 1–2-MHz region. Q_1 and Q_2 were matched Motorola MRF904's, and D_1 and D_2 were a Hamamatsu type S1722-01. The signal and comparison beam powers were 5.6 and 7.2 mW, respectively, and $i_{\text{signal}} = 1.77$ mA. The 5–100-kHz noise voltage spectral density averages $88.7 \text{ nV}/\sqrt{\text{Hz}}$, which (after accounting for $29\text{-nV}/\sqrt{\text{Hz}}$ instrument noise and a factor of 0.5 that is due to a $50\text{-}\Omega$ load) is within 0.15 dB of the predicted shot-noise level and shows a 1-Hz dynamic range of 154 dB. (a) dc to 100 kHz; the upper curve was taken in I - V (transresistance) mode (comparison beam blocked), the lower curve with the canceler operating normally. (b) 0 to 2 MHz; the top trace was taken in I - V mode, the middle curve with the canceler operating normally, and the bottom curve with both beams blocked (instrument noise).

by one multiplying all the gains together around the loop and setting the magnitude of the result to unity:

$$f_c = \frac{e}{2 \pi k T} \left[\frac{i_{\text{signal}}}{1 + \exp(e \Delta V_{\text{BE}} / k T)} \right] \frac{\gamma R_f}{RC}. \quad (7)$$

B. Performance

Figure 4 shows the performance attainable with the basic noise canceler of Fig. 3 in a system with photon efficiency (excluding detector quantum efficiency) $\eta \approx 1$. Q_1 and Q_2 were MRF904's, selected for good differential splitter performance by using a curve tracer. These devices have good log conformity, high speed, and low noise, but have betas of around 30,

which are often sharply peaked with collector current. Q_3 was an MPSA-64 as shown in Fig. 3. The photodiodes used were Hamamatsu type S1722-01, which are large-area (5-mm-diameter) PIN devices; these were chosen for good linearity at high photocurrents, at the expense of bandwidth. The feedback bandwidth was less than 100 Hz. The laser used here was a 40-mW, frequency-doubled, diode-pumped Nd:YAG unit. A diode laser or a gas laser (such as helium neon) would be equally suitable. The signal and comparison photocurrents were 1.77 and 2.16 mA, respectively, with optical powers of 5.6 and 7.0 mW; output was taken from A_1 , and the feedback resistor R_f was 5.11 k Ω . The large ratio of i_{C2}/i_{C1} (about 4) was chosen to reduce the transconductance of the differential pair, which reduces the extrinsic base resistance noise, as discussed below. The transresistance gain of the circuit is reduced by half here due to the $50\text{-}\Omega$ source and load impedances. The expected shot-noise voltage spectral density v_{ns} is $60.8 \text{ nV}/\sqrt{\text{Hz}}$ from signal current shot noise alone.

In each plot of Fig. 4, the output noise with the canceller running is compared with the noise with the comparison beam blocked, so that Q_2 is turned off, and the circuit operates as an ordinary transresistance amplifier. Figure 4(a) is an averaged plot of the input-referred noise spectral density from 0 to 100 kHz, while Fig. 4(b) shows the broadband noise level. The flatband noise spectral density after cancellation is $88 \text{ nV}/\sqrt{\text{Hz}}$, which is in excellent agreement with the expected value of $60.8 \sqrt{2} \text{ nV}/\sqrt{\text{Hz}} \approx 86.0 \text{ nV}/\sqrt{\text{Hz}}$; most of the remainder is contributed by the $29\text{-nV}/\sqrt{\text{Hz}}$ noise of the measurement system. This result represents a limiting dynamic range of 154 dB in 1 Hz, although over most of the usable range of ΔV_{BE} , the base-spreading resistance noise will limit its dynamic range to approximately 150 dB in 1 Hz, as already noted. The resulting noise has Gaussian statistics, even far out in the wings of the Gaussian; considered as an imputed error in its variance, the deviation is less than 0.1 dB out to 7σ or more, even with a mode-hopping diode laser.¹⁷

Figure 5 contains frequency response plots of the ultimate cancellation performance of the prototype. The beam was amplitude modulated by a few parts in 10^3 before splitting by the spectrum analyzer's tracking generator driving a Pockels cell, with an analyzer to convert the resulting polarization shift to amplitude modulation. The data are from a spectrum analyzer; one sweep was taken with the canceller operating normally and a second sweep with the comparison beam blocked. The cancellation behavior depends on the ratio of the comparison and signal beam powers. The bandwidth of the amplifier A_1 was only 1.4 MHz and that of the feedback less than 100 Hz. The ultimate cancellation was nearly 60 dB to 100 kHz and deteriorated to 40 dB at approximately 1 MHz, primarily owing to the capacitance of the photodiodes (which seems to become worse at high light intensities) and the relatively poor high-frequency behavior of Q_3 . By

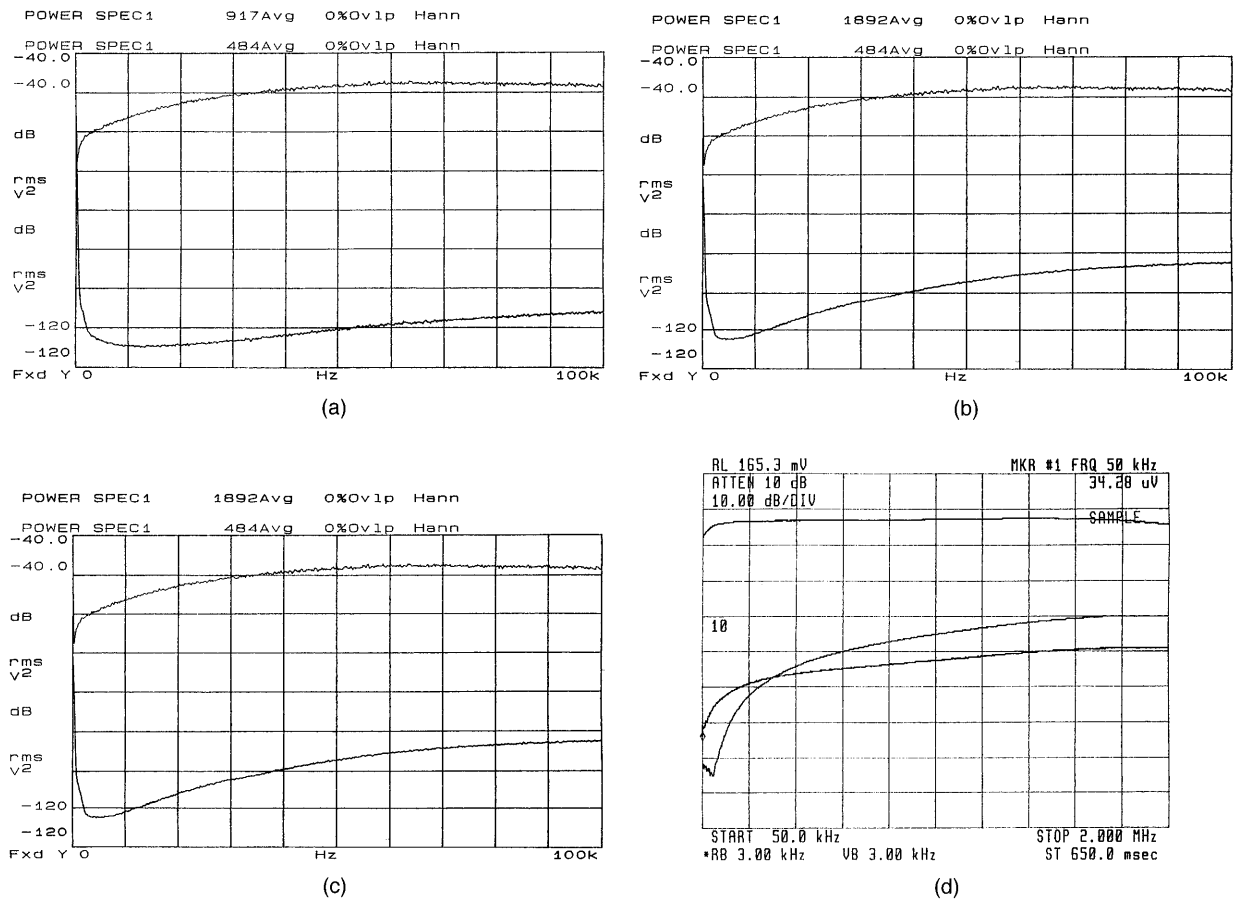


Fig. 5. Frequency response of the ultimate cancellation performance of the same canceller used in Fig. 4 with small (0.3%) intensity modulation. The signal beam power was 1.86 mW and $i_{\text{signal}} = 0.583$ mA. In (a)–(c), the top curve was taken in I - V mode and the bottom curve with the canceller operating normally. This canceller version is optimized for good cancellation at the highest collector currents and low frequencies. (a) $V_{\text{log}} = +1.88$ V ($i_{\text{comp}} \approx 1.4i_{\text{signal}}$). The cancellation is 55–60 dB throughout the baseband range shown. (b) $V_{\text{log}} = 0.38$ V ($i_{\text{comp}} \approx 1.83i_{\text{signal}}$). The cancellation is not as good at this setting. (c) $V_{\text{log}} = -0.145$ V ($i_{\text{comp}} \approx 2.08i_{\text{signal}}$). The cancellation is seriously degraded at this value of the comparison current. (d) 50-kHz, 2-MHz cancellation response showing the effect of the choice of comparison current on the ac response. Bottom right trace: $V_{\text{log}} = 2.70$ V ($i_{\text{comp}} \approx 1.25i_{\text{signal}}$); bottom left trace: $V_{\text{log}} = 0.394$ V ($i_{\text{comp}} \approx 1.82i_{\text{signal}}$). Note the effect on the cancellation bandwidth of starving Q_1 of collector current.

changing Q_3 to an MM4049, selected for good beta linearity, and reducing the beam power somewhat, the high-frequency situation can be improved a good deal, as shown in Fig. 6. The result in Fig. 6(b), where the cancellation is as great as 40 dB out to a modulation frequency of 10 MHz, is as good as a dominant-pole feedback stabilizer with a bandwidth of 1 GHz.

C. Effects of Nonideal Transistors

Real transistors do not follow the Ebers–Moll model exactly, and their collector currents are not exact replicas of their emitter currents. The most important sources of error are the emitter bulk (extrinsic) resistance r_E and beta nonlinearity.

To achieve perfect cancellation, the collector current of Q_1 must be exactly proportional to the comparison photocurrent i_{comp} . The small-signal

(differential) current gain of a transistor is

$$h_{fe} = \frac{\partial i_C}{\partial i_B}, \quad (8)$$

while the large-signal (average) current gain is

$$h_{FE} = \frac{i_C}{i_B}. \quad (9)$$

These two gains in general are not equal, which causes the fluctuations in the comparison photocurrent to split differently between the collector and base than the dc average; this degrades the attainable cancellation. In the absence of other effects, the lower limit imposed by beta nonlinearity on the uncanceled fraction of the noise with a given transistor is equal to the proportion of the emitter current of Q_2

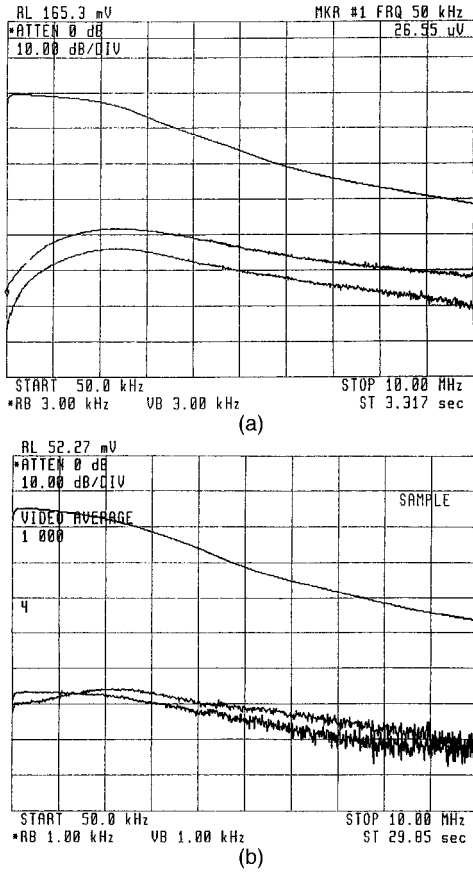


Fig. 6. 50-kHz to 10-MHz frequency response of the ultimate cancellation performance of the canceller used in Fig. 5 with the exception that Q_3 here is a MM4049 rf device selected for good beta linearity and that the circuit is operated at lower current. In each plot, the top trace is the beam modulation, made in I - V mode. (a) $i_{\text{signal}} = 0.235$ mA. Middle trace: $V_{\text{log}} = 2.87$ V ($i_{\text{comp}} \approx 1.24i_{\text{signal}}$); bottom trace: $V_{\text{log}} = 0.388$ V ($i_{\text{comp}} \approx 1.82i_{\text{signal}}$). The deterioration of the cancellation with frequency is less rapid than in Fig. 5, and the low-frequency cancellation behavior is better as well—almost 70 dB. (b) $i_{\text{signal}} = 0.153$ mA. Middle trace: $V_{\text{log}} = +0.296$ V ($i_{\text{comp}} \approx 1.86i_{\text{signal}}$); bottom trace: $V_{\text{log}} = 0.00$ V ($i_{\text{comp}} \approx 2.00i_{\text{signal}}$). Poorer low-frequency behavior is offset by excellent high-frequency response, although A_1 's bandwidth is only 1.8 MHz and the feedback bandwidth <100 Hz, the cancellation is >50 dB to 2 MHz, and >40 dB to at least 8 MHz, where the cancelled signal drops below the shot-noise floor (1 kHz BW).

that goes out the wrong lead:

$$A_{\min} = \frac{1}{h_{FE}} \left| 1 - \frac{h_{FE}}{h_{fe}} \right|. \quad (10)$$

Thus the best devices will have large betas that are not strong functions of i_C . This limitation is especially awkward when rf transistors are used because their betas tend to be low and quite strongly peaked with i_C .

Another source of error is degenerative (negative) feedback to the emitters caused by the emitter bulk resistance r_E of the transistors. This feedback depends on the values of the collector currents of Q_1 and Q_2 , so that their transconductances are no longer

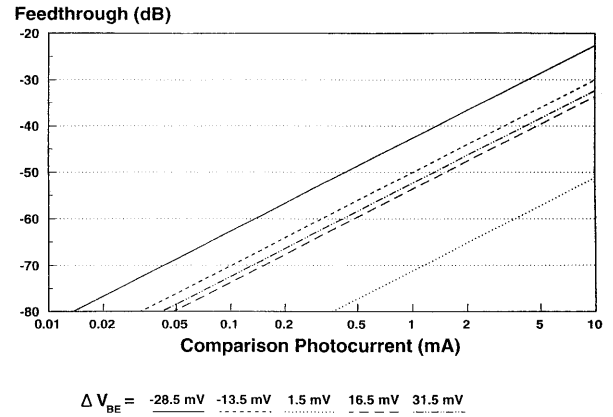


Fig. 7. Calculated limit to cancellation performance that is due to equal $0.5\text{-}\Omega$ emitter bulk resistances r_E in Q_1/Q_2 as a function of ΔV_{BE} and i_{signal} .

proportional to their collector currents; this causes the fluctuations in i_{comp} to split differently than the dc. The limit on cancellation performance set by r_E is equal to the proportion of the fluctuations that goes to the wrong collector:

$$A_{\min} = \frac{\left| \frac{\partial i_{C2}}{\partial i_{\text{comp}}} - \frac{i_{C2}}{i_{\text{comp}}} \right|}{\frac{i_{C2}}{i_{\text{comp}}}}. \quad (11)$$

In Appendix A, this is shown to be (to leading order in eir_E/kT):

$$A_{\min} \approx \frac{e}{kT} \frac{(i_{\text{sample}} - i_{\text{signal}})}{i_{\text{sample}}} \times [r_{E1}(i_{\text{sample}} - i_{\text{signal}}) - r_{E2}i_{\text{signal}}]. \quad (12)$$

The limit depends on ΔV_{BE} and on collector current. Figure 7 shows the effects of r_E as a function of collector current and ΔV_{BE} for small-signal transistors with $r_E \approx 0.5 \Omega$. Figure 8 shows the cancellation performance of the circuit of Fig. 5 at a frequency of 1 kHz for a variety of signal currents. Figure 9 shows the experimental curves for a temperature-controlled MAT-04 transistor array, showing the much more predictable behavior of this device, which is due to its better beta linearity and freedom from temperature drifts.

Besides these limits due to r_E and beta nonlinearity, there is the Johnson noise contributed by the base spreading resistance r_b , typically $40\text{--}100 \Omega$ for small-signal devices, which contributes an ultimate noise floor of approximately $1 \text{ nV}/\sqrt{\text{Hz}}$ on each base. Near null, this corresponds to a voltage SNR of $(2kT/e)/1.4 \text{ nV}$ (about 150 dB) in 1 Hz, equivalent to the total system shot noise with a photocurrent of $800 \mu\text{A}$ (signal beam power of approximately 2.7 mW). This effect can be reduced by operating the circuit with a fairly small comparison beam, which forces ΔV_{BE} to be positive, reducing the transconductance of Q_1 and hence that of the stage; by choosing a tran-

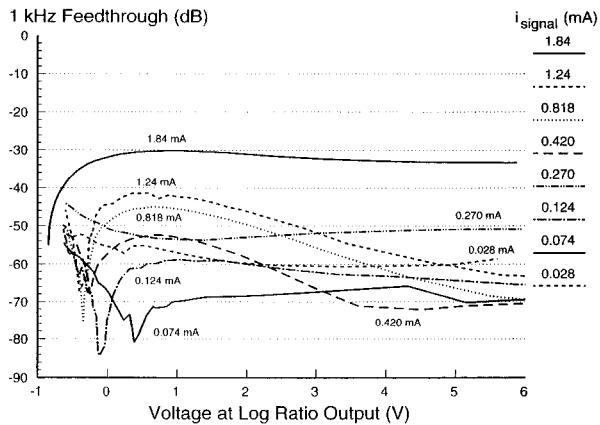


Fig. 8. Measured 1-kHz cancellation performance of the circuit of Fig. 3 as a function of the log ratio output voltage that reflects $i_{\text{comp}}/i_{\text{signal}}$. The green Nd:YAG laser beam was sinusoidally modulated at 1 kHz by using an acousto-optical modulator, a variable attenuator, a Glan–Taylor prism to control the polarization, a Wollaston prism to split the beams, and a rotatable Glan–Thompson prism in the comparison beam to adjust the relative beam intensities. All were slightly misaligned to control étalon fringes. The interaction of r_E degeneration and beta nonlinearity make the details of the cancellation performance difficult to predict *a priori*, but there is a clear trend toward better cancellation at lower currents.

sistor type with low r_b ; by paralleling devices to reduce the effective value of r_b ; by reducing the transconductance of the differential pair by diode degeneration, as shown in Subsection 4.A; or by using the differential/high-dynamic-range version of the noise canceller, where i_{C2} is a small fraction of the total signal photocurrent. The Thévenin resistance of the voltage divider used on the base of Q_2 also contributes noise, so care should be taken to keep it below r_b . Because the transconductance of a BJT increases with collector cur-

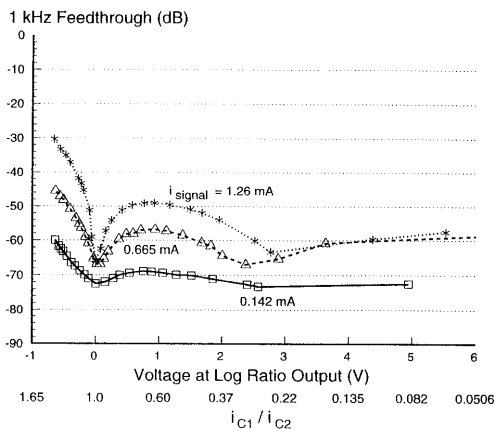


Fig. 9. Cancellation performance at 1 kHz of the circuit of Fig. 3 with a temperature-stabilized MAT-04 matched array used for Q_1 and Q_2 . Excellent beta linearity of this device and elimination of temperature errors result in much more predictable cancellation performance. The deep minima near 0 V are due to symmetric cancellation of r_E degeneration. The sharp deterioration with negative V_{log} is due to the rapidly increasing current in Q_1 , which increases its r_E nonlinearity.

rent, r_E degeneration and r_b noise become more serious limitations as the laser power increases. This means that with the basic noise canceller of Fig. 3, the signal-to-shot-noise ratio of the data cannot be increased indefinitely by increasing laser power. With heterodyne techniques—providing that the signals are weak enough that noise intermodulation does not set the noise floor—the SNR can in principle always be increased by increasing laser power.

The f_T of the transistors also is a function of collector current; it usually exhibits a broad peak somewhat below the maximum rated i_C and decreases steadily with decreasing i_C below there. Because the cancellation bandwidth depends on f_T , the best bandwidth performance will be obtained usually with transistors run at collector currents not less than about 1% of their maximum rating.

Large splitting ratios force Q_1 to operate at low collector current and thus reduce its f_T , which may limit the high-frequency performance of the circuit; this effect can be mitigated by one choosing transistors such as the MRF9331, which has excellent speed at low collector currents.

4. Circuit Variations

A. Variation 1: Low-Noise Floor

There are situations in which the SNR needs to be increased further, but the laser power cannot be increased. This may be due to dose limits, as in measurements on undeveloped photoresist or biological specimens or cost constraints. In this case careful optimization is necessary to achieve the best possible performance.

By introducing N ideal diodes into each emitter, one can reduce the shot-noise contribution of the Q_1/Q_2 pair without sacrificing cancellation performance. Although the diodes contribute shot voltage noise of their own, nevertheless the degenerative feedback reduces the overall shot noise contributed by the current splitter by a factor of $(N + 1)^{-1/2}$. With enough diodes in series, the split current will have almost the same signal-to-shot-noise ratio as the total comparison current. If the comparison photocurrent is several times larger than the signal current, this represents a large improvement over the 3 dB discussed above. If the $i_{C1} = 4i_{\text{sig}}$, its signal-to-shot-noise ratio will be 6 dB higher. Because of the transconductance reduction, the emitter degeneration from the additional bulk resistance contributed by the diodes need not be a limitation. In Appendix A, it is shown that with N diodes in series with each emitter, the total noise current contributed by the comparison photocurrent and differential pair becomes

$$\langle i_{n2} \rangle^2 = 2ei_{C2} \left(1 - \frac{N}{N+1} \frac{i_{C1}}{i_{C1} + i_{C2}} \right). \quad (13)$$

If the circuit is modified as shown in Fig. 10, and the comparison current made five times larger than i_{signal} (so that 80% flows to ground), the shot noise in

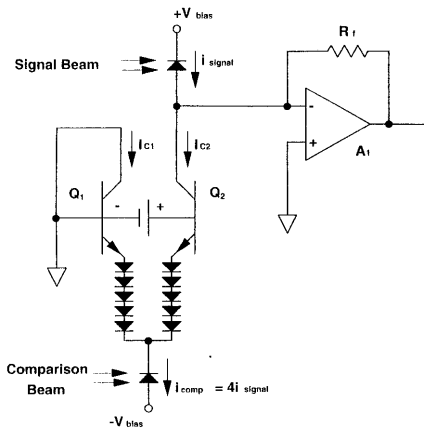


Fig. 10. One implementation of low-noise current splitting, to reduce the 3-dB noise penalty resulting from the uncorrelated shot noise of i_{C2} and i_{signal} . With $i_{\text{comp}} = 5i_{\text{signal}}$, the noise degradation resulting from i_{comp} is now a factor of 1.33 (1.25 dB) instead of 2 (3 dB) and can be reduced further by one increasing the relative size of the comparison beam.

the final split comparison current is still 4.8 dB less than that in the signal current, and the 3-dB penalty is reduced to 1.25 dB, a 1.75-dB improvement. A splitting ratio of 9:1 and 10 diodes per side reduces the penalty by another half decibel to 0.72 dB.

Figure 11 shows the improvement in performance obtained by using this circuit, with diode-connected MAT-04's used as the emitter diodes. (This is necessary, because real diodes do not obey the diode equation, whereas diode-connected transistors do.) The signal current was 0.189 mA (corresponding to a signal beam power of 0.61 mW) and the ratio $i_{\text{comp}}/i_{\text{signal}}$ was 5.0. The noise improvement is 1.7 dB, which is in excellent agreement with the expected value of 1.75 dB from Eq. (13).

The performance level reached by the basic (Fig. 3) noise canceler is the same as that of an ideal heterodyne system because the 3-dB extra noise resulting

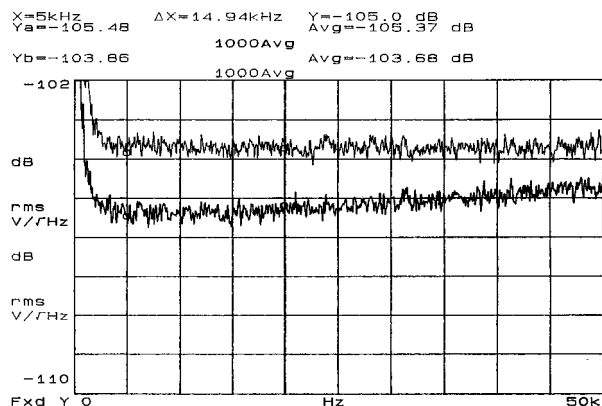


Fig. 11. Noise floor of the low-noise canceller of Fig. 10 compared with that of Fig. 4. Q_1 and Q_2 were part of a MAT-04 array, with five diode-connected (base and collector shorted) MAT-04 devices in each emitter. The value of i_{signal} was 0.189 mA and $i_{\text{comp}}/i_{\text{signal}}$ was 5.0. The noise floor is 1.7 dB lower, in excellent agreement with the expected value of 1.75 dB calculated from Eq. (13).

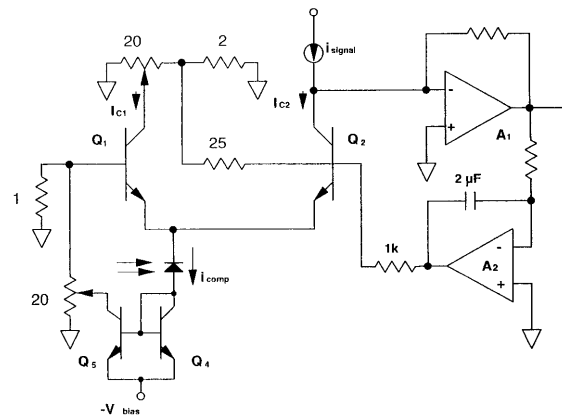


Fig. 12. Application of regenerative feedback to the bases of Q_1 and Q_2 for r_E compensation.

from the comparison beam shot noise is balanced by the factor of 2 decrease in bandwidth of homodyne or dual-beam measurements compared with heterodyne ones with the same temporal response. It is superior to that of an ideal chopped system because chopers exhibit 3-dB additional loss owing to a 50% duty cycle. The present variation achieves a noise level 1.7 dB better than the best heterodyne system.

B. Variation 2: High Spurious Suppression

Some lasers exhibit strong spurious signals that are spectrally narrow so that the power spectral density within the spur is very high; examples include power supply ripple and baseband mode beats in gas lasers. In such cases, enough of the spurs may remain after cancellation with the basic circuit to be bothersome. Since the effectiveness of the cancellation is limited by beta nonlinearity and emitter bulk resistance in the differential pair, we seek methods for compensating for their effects.

The emitter bulk resistance r_E of a transistor appears in series with the emitter. Here it applies degenerative feedback to the emitters of Q_1 and Q_2 , causing their transconductances to deviate from the predictions of the Ebers-Moll model. This degeneration can be compensated for by applying regenerative feedback to the bases so that the base-to-intrinsic-emitter bias is restored to the ideal value. The required bias is

$$\Delta V_{\text{comp}} = r_{E2}i_{C2} - r_{E1}i_{C1}, \quad (14)$$

where the second-order term in $i_E - i_C$ is neglected. We form the correction term as

$$\Delta V_{\text{comp}} = -i_{C1}(r_{E2} + r_{E1}) + i_{\text{comp}}r_{E2}, \quad (15)$$

which is implemented as shown in Fig. 12. The i_{C1} term is obtained directly, the i_{comp} term from a current mirror (for biasing reasons). Adjustment is accomplished by shunting part of the currents to ground via the potentiometers. As the r_E term is small, the additional shot noise contributed by the current mirror is inconsequential.

Compensating for beta nonlinearity is more diffi-

cult. The replacement of Q_3 with a Darlington pair of fast transistors or a field-effect transistor (FET) may help, but Q_1 and Q_2 cannot be replaced this way. FET differential pairs are ruled out because they do not obey Eq. (3), Darlington pairs because of their poor transconductance linearity. The best course is to choose simple BJT devices with high beta and good linearity for Q_1 and Q_2 . The Analog Devices MAT-04 transistor arrays used here are excellent in this regard, although their f_T 's are relatively low, especially for collector currents below 0.2 mA. The NEC UPA10x series of transistor arrays are claimed to have extremely high beta linearity, along with gigahertz f_T 's, and are under evaluation. If discrete devices are to be used, small-signal PNP devices generally have better beta linearity than NPN's, but significantly worse r_E , so better performance at low beam powers may sometimes be obtained by one inverting the polarity of the entire circuit. Care must be taken with discretely, however, because even small temperature differences between transistors can limit cancellation performance at this level. Figure 13 shows the improvement in the cancellation performance when r_E compensation is applied to a MAT-04 and demonstrates the possibility of one achieving as much as 28-dB improvement over the basic circuit of Fig. 3 at high current levels. A MPSA64 Darlington transistor was used for Q_2 to avoid beta nonlinearity effects there; the flatness of the compensated curves suggests that the predominant limitation at this level is the beta linearity of Q_2 . The improvement declines at lower current levels, as expected, but it is apparent that the low-current performance is not degraded significantly by the r_E compensation circuitry. Because this method is capable of producing upward of 70 dB of cancellation (even with large signals), even minor departures from ideal conditions can degrade the overall system performance. Stray light, vignetting, photodiode response nonuniformity, and incidental étalon fringes can be serious problems. It also requires two trims and is mildly sensitive to the exact value of the photocurrents. Nevertheless, for high-dynamic-range, single-ended measurements with noisy lasers, it provides a level of performance otherwise unobtainable.

C. Variation 3: Ratio Only

In situations such as spectroscopy, in which only a normalized output is desired, it is possible to eliminate A_1 entirely to achieve a wider feedback bandwidth and somewhat better suppression on the logarithmic output, as shown in Fig. 14.¹⁵ The control voltage is now applied to the base of Q_1 , since the elimination of A_1 inverts the sign of the loop gain. The loop bandwidth f_c is as given in Eq. (7), with $R_f = R$ and the sign of ΔV_{BE} inverted, and the output noise level is given by Eq. (6) with the sign of ΔV_{BE} changed. Figure 15(a) shows the noise floor of the present version (averaged from 3 to 10 kHz) as a function of i_{signal} for two values of ΔV_{BE} . The noise floor is within 1 dB of the predicted value, and the limiting 1-Hz SNR near null is indeed approximately

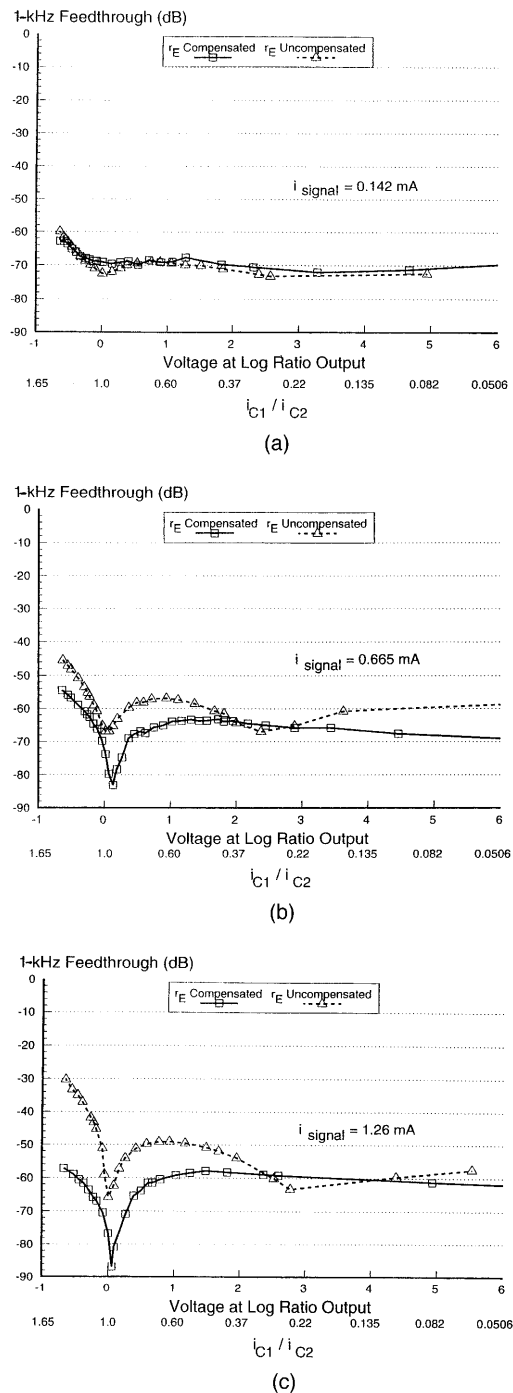


Fig. 13. Cancellation performance of the high spurious suppression canceller of Fig. 12 (solid curve), under the same conditions as in Fig. 9, as a function of the strength of i_{C2} . The data of Fig. 9 (dashed curve) are provided for comparison. The compensation circuit makes the behavior of the canceller stable over a wide range of signal and comparison currents. (a) $i_{\text{signal}} = 0.142$ mA. The curves are nearly identical because r_E is not a significant limitation yet. (b) $i_{\text{signal}} = 0.665$ mA. The compensated device is several decibels better nearly everywhere and as much as 15 dB near null. (c) $i_{\text{signal}} = 1.26$ mA. The benefits of r_E compensation become evident, with as much as 28-dB improvement. Cancellation is >60 dB almost everywhere.

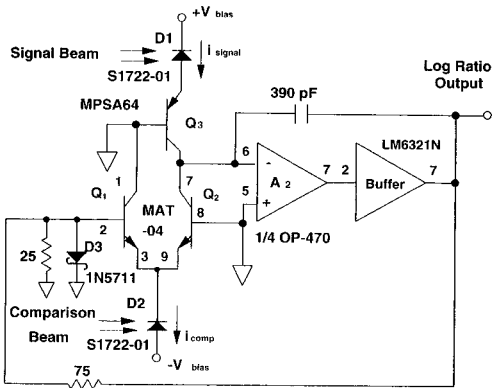


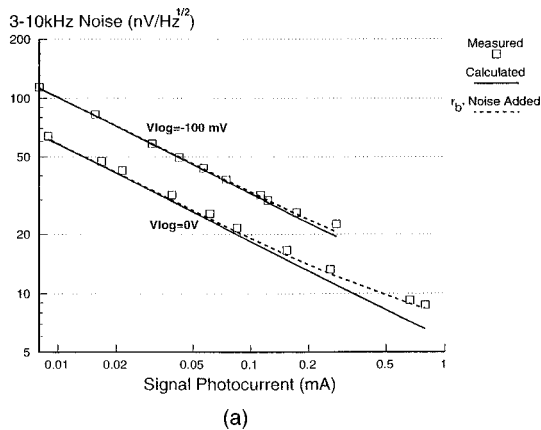
Fig. 14. Ratio-only version of the noise canceler. The photocurrent now goes directly to the summing junction of A_2 . The time constant of A_2 has been reduced. Feedback goes to the base of Q_1 now, since the sign of the loop gain was changed by the elimination of inverting amplifier A_1 . Schottky diode D_3 protects Q_1 from excessive base currents when A_1 is saturated.

150 dB, as predicted; the highest power signal corresponds to a noise voltage of $9 \text{ nV}/\sqrt{\text{Hz}}$ and a scale factor of 220 mV, a 1-Hz SNR of 147 dB. Figure

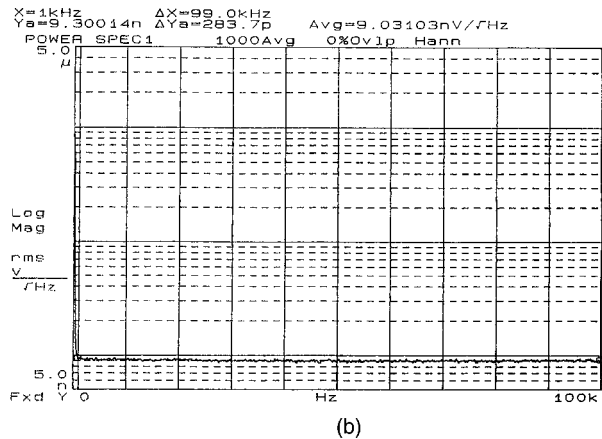
15(b) shows 0–100-kHz noise floor corresponding to the rightmost point on the lower curve of Fig. 15(a). The noise is very flat and well behaved even in the low audio frequency range. Figure 15(c) shows the frequency response of the ratio-only version for two values of i_{signal} . Even with beam powers of only a few hundred microwatts, bandwidths of a few megahertz are easily achieved. Figure 15(d) is a swept-sine plot of the cancellation performance of this variation, which shows performance similar to the others.

A disadvantage of the ratio-only variation is that it is no longer possible to obtain an uncanceled (I - V mode) signal simply by blocking the comparison beam; however, a switch can easily be added to change the feedback capacitor for a resistor and break the feedback loop.

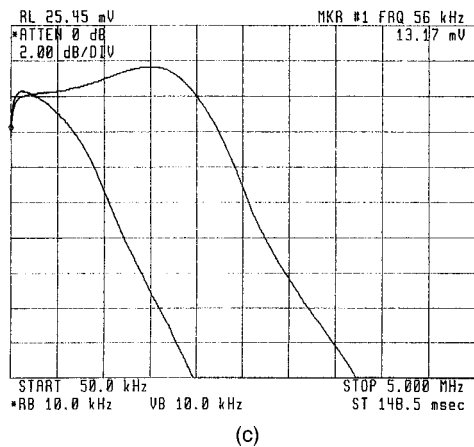
Another approach, which is adopted in Figs. 18(c) and 19, is to block one of the beams, in this case the signal beam, and use another light source, such as a light-emitting diode or a flashlight, to provide the photocurrent. Because of the large variations in the gain of the log ratio output, it is vital to ensure that the replacement light power is the same as the original beam; this is done by one adjusting the replace-



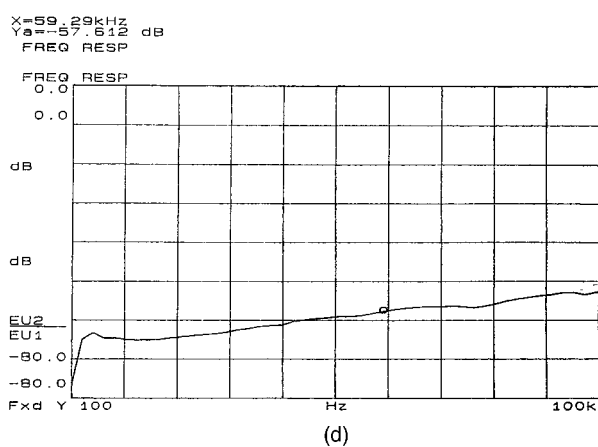
(a)



(b)



(c)



(d)

Fig. 15. Noise floor and frequency response of the ratio-only noise canceller of Fig. 14. (a) Flatband (3–10 kHz) noise voltage spectral density compared with the prediction of Eq. (6) (with the sign of ΔV_{BE} inverted). (b) Noise floor with $V_{A2} = 0.00 \text{ V}$, with $i_{\text{signal}} = 931 \mu\text{A}$ (corresponding to the rightmost point of the lower curve in (a)). The flatband extends down to the low audio frequencies. (c) Differential signal frequency response of the ratio-only noise canceller with an incandescent light supplying the comparison current so that all the modulation appears as signal (see text). V_{A2} was 0.00 V . (d) Swept sine cancellation behavior at null ($V_{A2} = 0.000 \text{ V}$).

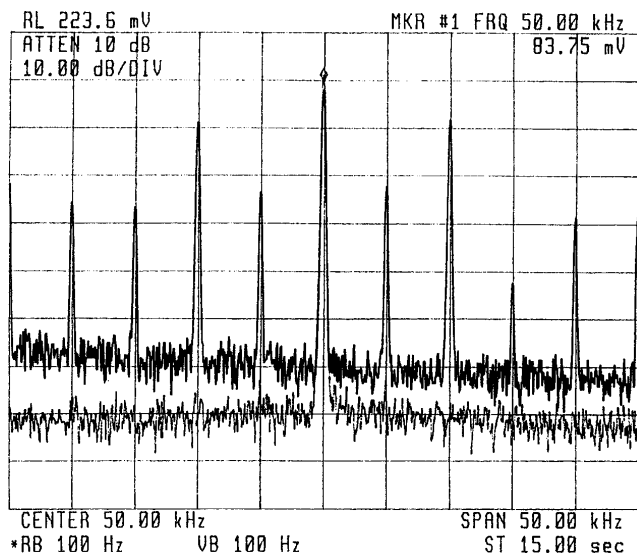


Fig. 16. Noise intermodulation suppression performance of the ratio-only noise canceller of Fig. 14. This measurement was made with the apparatus of Fig. 15 and arranged so that the Pockels cell and Glan-Taylor combination produced a harmonic-rich 5-kHz common-mode modulation of approximately 30% p-p. A liquid-crystal ferroelectric modulator was put in the comparison beam to provide a differential signal. The liquid-crystal modulator was driven with a small amplitude sine wave at 50 kHz to produce a sinusoidal modulation 0.3% p-p. The result is a 50-kHz differential optical modulation that has large modulation sidebands at harmonics of 5 kHz (upper trace: comparison beam blocked, incandescent lamp supplying i_{comp}). When the comparison beam was unblocked (lower trace: same i_{comp}), the strong 5-kHz intermodulation peaks essentially disappeared.

ment light intensity until the dc voltage at the log ratio output is the same as with the original beam.

To those workers desiring the widest possible log ratio bandwidth, one note of caution is in order. Because the bandwidth goes as i_{signal} and the output noise power density goes as i_{signal}^{-1} , the total noise at the log ratio output is independent of i_{signal} , depending only on the integrating capacitor and the voltage divider ratio. For the ratio-only canceler to function properly, the total rms noise voltage at the base of Q_1 must be much less than kT/e . If the capacitor chosen is too small, significant noise intermodulation may occur, which will reduce the performance of the device. Capacitances of at least 10 pF should give good results (with fast amplifiers). Small capacitors may also cause the loop to become unstable at large values of i_{signal} if the rest of the circuit is too slow.

Since the voltage divider ratio γ will be larger here than in Fig. 3 (for increased bandwidth, while still reducing the noise of A_2), a Schottky diode shunting the base of Q_1 to ground is included. This prevents damage to the transistor from excessive base-collector current when A_2 is saturated.

Provided the beam powers do not vary too much (no more than 2:1, say), it should be possible to achieve significantly better medium-frequency loop gain—and hence better noise intermodulation

suppression—with lead-lag frequency compensation.

Figure 16 shows the intermodulation suppression of the log ratio canceller of Fig. 14. The experimental setup used a Pockels cell and a Glan-Taylor prism to modulate the laser beam by approximately 30% at 5 kHz. The resulting amplitude modulation had a severely distorted envelope that was due to the non-linearity of the Pockels cell-polarizer combination, so that its modulation spectrum was rich in harmonics of 5 kHz. The resulting beam was split by a Wollaston prism. One of the two resulting beams (the cancellation beam here) was further modulated by approximately 0.1% at 50 kHz with a liquid-crystal variable retarder and a film polarizer. The upper trace of Fig. 16 was taken with a flashlight to replace the signal beam, as discussed above, whereas the lower trace was taken with the canceler operating normally. The 50-kHz carrier is preserved, even increased slightly by the return of the sideband energy, but the very strong, harmonic-rich 5-kHz modulation is suppressed by more than 60 dB. (The small residual peaks at ± 5 kHz, whose spectrum is different from the amplitude modulation spectrum of the upper trace, seem to be due to phase modulation of étalon fringes from the stray light, although straight feedthrough is not ruled out.) The noise intermodulation suppression of this technique is superior to any previous method. This feature makes possible accurate extinction measurements with lasers whose power varies greatly during a scan, such as current-tuned diode lasers. By the elimination of the large ramp signal that is due to the laser intensity change, this device makes possible such measurements as ultrasensitive tunable diode laser spectroscopy with a simple dual-beam approach. It is currently used in tunable diode laser measurements of the oxygen content of the Earth's atmosphere.

Because the gain and dc level at the log ratio output depends on the temperatures of the differential pair Q_1 - Q_2 , some sort of temperature compensation or stabilization is required. It is possible to make efforts at temperature compensation of this output, for example by the use of forward-biased diodes connected in shunt with the bases of Q_1 and Q_2 (as is commonly done in integrated circuit operational transconductance amplifiers such as the LM13600²⁴) or by the use of thermistors; however, the best way to do it is to temperature stabilize the circuit to eliminate the temperature variations themselves. Ovenizing the entire circuit is awkward, but adequate performance can be obtained by stabilizing the differential pair alone, an idea sometimes used in logarithmic amplifiers.²⁵

Figure 17 shows a circuit fragment to control the temperature of the differential pair right on the die. Differential pair Q_1 and Q_2 are two diagonally opposite sections of a monolithic quad transistor, such as the Analog Devices MAT-04 or NEC UPA104. Of the other two sections, Q_3 functions as a diode temperature transducer and Q_4 as a heater. The feedback loop forces the V_{BE} of Q_3 to be 90% of its room-

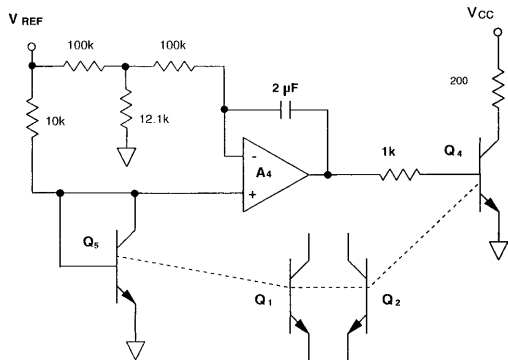


Fig. 17. On-chip temperature stabilization of Q_1/Q_2 , which are diagonally opposite sections of a MAT-04. Of the other two sections, Q_5 is a temperature sensor and Q_4 a heater. The design temperature is 330 K with a reference voltage of approximately 5 V.

temperature value; because this voltage is inversely proportional to temperature, this ensures that Q_1 and Q_2 operate at a fixed temperature of approximately 330 K and so practically eliminates temperature drift as a source of error.

Technical problems such as incidental étalon fringes can be severe in this sort of measurement; a 1-mm-thick window of antireflection-coated BK-7 glass (1% reflection per interface) used at 632.8 nm exhibits fringes that can cause a drift in the apparent extinction of $1 \times 10^{-3}/^\circ\text{C}$ from thermal expansion of the glass, as well as 3.8% per wave number in frequency. Longer étalons and stronger reflectors are correspondingly worse.

Figure 18 shows the drift performance of the temperature-controlled ratio-only version, combining Figs. 17 and 19, in a metal box in ordinary laboratory conditions with windowless photodiodes. No other temperature stabilization or insulation was used.

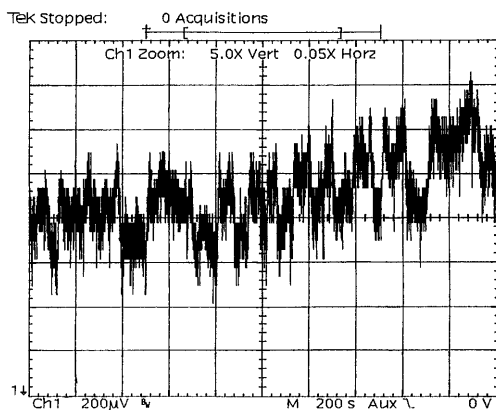


Fig. 18. Drift performance of the temperature-controlled ratio-only noise canceller of Figs. 17 and 19, run in a small uninsulated metal box with windowless photodiodes to control étalon fringes in the setup used in Fig. 9. The signal and comparison beam powers were 1.25 and 2.50 mW, respectively. The Hamamatsu S1722-01 photodiodes were inadequately passivated for windowless operation, as shown by the strong popcorn noise, which was not observed with the photodiode windows intact. Scale: 10^{-4} extinction/div vertical, 200 s/div horizontal.

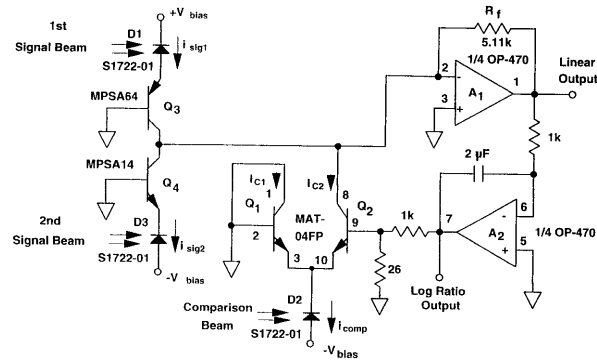


Fig. 19. Schematic of the differential and high-dynamic range noise canceller. A second signal photodiode D_3 and transistor Q_4 are added to Fig. 3. Photocurrent $i_{\text{sig}1}$ is made slightly (perhaps a few percent) larger than $i_{\text{sig}2}$. Most of the photocurrent flows from D_1 to D_3 , leaving all of the desired signal, the shot noise, and a reduced dc current. The differential pair operates at lower current, reducing the effects of r_b , noise, i_{C2} shot noise, and r_E non-linearity, so the limiting SNR closely approaches the signal-to-shot-noise ratio of the two strong beams.

The optical system was the same green Nd:YAG laser used before, with a Wollaston prism used for the beam splitting. These diodes were the same Hamamatsu units used before, with the windows removed. Because of their poor passivation, they exhibited strong $1/f$ noise in the presence of environmental contamination, resulting in the popcorn noise characteristic of Fig. 18. The drift results depend to a considerable degree on ambient conditions, such as thermal gradients and air currents, but these results with this setup show stabilities of approximately 1 part in 10^4 over an hour or so.

D. Variation 4: Differential High Dynamic Range

Many of the most sensitive optical measurements are made in differential systems where the signal desired is the difference between the intensities of two beams. In such cases, the circuit of Fig. 19 is useful. It has two signal photodiodes; $i_{\text{sig}1}$ is made slightly larger than $i_{\text{sig}2}$, so that the differential pair must always sink at least some current to keep the circuit in balance.

The two signal photocurrents $i_{\text{sig}1}$ and $i_{\text{sig}2}$ are subtracted directly by putting the signal photodiodes in series (with cascode transistors as before), which eliminates the phase and gain error problem, and the (small) comparison current goes through the differential pair Q_1/Q_2 . Because the current imbalance is assumed to be small, i_{comp} can be kept small, and so the additional noise and error introduced are small as well. Figure 20 shows the improved performance of this version. Even with a total signal beam power of over 10 mW, 70 dB of low-frequency cancellation can be achieved without adjustments, and significantly more with occasional manual tweaking of the beam position on the photodiodes. This result should be compared with those of Fig. 8 for the single-ended model. High-frequency cancellation performance

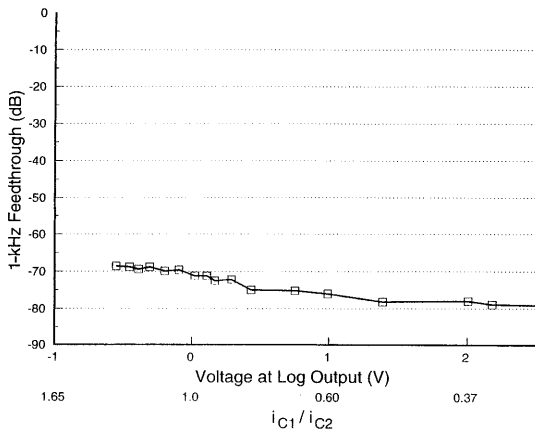


Fig. 20. Cancellation performance of the differential circuit of Fig. 19 at 50 kHz. The data are the ratios of the residual 50 kHz at the output of A_1 with the canceler operating to the total 50-kHz power in both beams combined ($i_{\text{sig}1} = 1.48$ mA, $i_{\text{sig}2} = 1.36$ mA). The cancellation performance is nearly independent of the comparison beam power, in contrast to the situation of Fig. 8, even though the total signal photocurrent is twice as great as that of the worst performing trace of Fig. 8.

improves somewhat less, as the component speed is still a limiting factor.

There are situations, especially with powerful lasers, in which excess noise must be reduced to levels below the ultimate noise floor of the basic noise canceller. The differential noise canceller is especially suited to this situation. Because the two signal photocurrents can be large compared with the comparison current (provided the maximum imbalance in the signal currents is sufficiently low), the collector currents of the differential pair can be kept small, for good cancellation performance and low r_b noise, while the signal currents can be made as large as necessary for the best SNR, within the limitations of the components used.

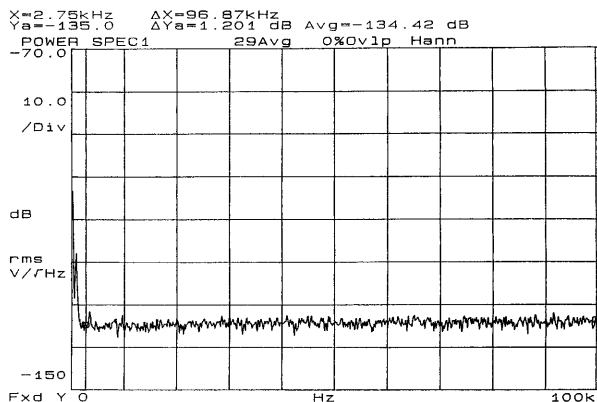


Fig. 21. Noise floor of the differential noise canceller of Fig. 19 ($i_{\text{sig}1} = 1.83$ mA, $i_{\text{sig}2} = 1.77$ mA, $i_{\text{comp}} = 0.15$ mA). The total signal beam power was 14 mW. The available signal from A_1 is 18.6 V, or +25.4 dBV. The measured 3–100-kHz noise voltage spectral density is -134.4 dBV rms/Hz or -134.6 dBV rms after correction for the 30-nV/ $\sqrt{\text{Hz}}$ instrument noise. The 1-Hz SNR is thus 160.0 dB.

Figure 21 shows the noise floor of the present version, operating with a total signal beam power of 14 mW and exhibits a 1-Hz SNR of 160 dB, approximately 0.5 dB less than the theoretical value. This corresponds to a measurement uncertainty of 7 parts in 10^9 in 1 s, even at the baseband. The effects of transistor nonlinearity and noise have been essentially eliminated here.

For single-ended measurements demanding such dynamic range, one of the signal inputs can be used as a second, higher-power comparison input that does not suffer from the nonideal behavior of Q_1/Q_2 .

In a system demanding the highest dynamic range, it is vital that the current density in the photodiodes be kept sufficiently low. High-current densities lead to flattening of the potential gradient in the junction, causing nonlinearity resulting from intensity-dependent photocarrier recombination rates. Solar cells work well at very high current densities, but this technological sophistication seems slow to appear in signal photodiodes.

E. Performance Optimization in Operation

Whichever version is used, there are a few things to remember when using the noise canceller. The most important is that it removes the bulk of the laser amplitude noise. This (while a virtue) makes prominent some seldom-considered second-order effects, which can limit the performance of the experiment if care is not taken. These effects include the noise of the unpolarized spontaneous emission, spatial dependence of the laser noise, photodiode response non-uniformity, and étalon fringes.

The noise canceller cancels only the correlated part of the noise, so for best performance both photodiodes must see exactly the same mode spectrum. In practice, this means putting an efficient polarizer in front of the laser to eliminate spontaneous emission in the orthogonal polarization state—this will in general not be split in the same ratio as the laser light by the beam splitter—and making sure that none of the beams spills off the photodiodes or is otherwise vignetted.

In many lasers, the noise spectrum depends on the detector's position in the beam, so special care must be taken to avoid any vignetting (this effect is particularly strong in diode lasers, even single-longitudinal mode types). If the spatial dependence of the laser noise is strong, the nonuniformity (typically 1–5%) of the responsivity of the photodiodes can cause degraded cancellation; this can be improved by one moving the beams around on the photodiodes while watching the noise floor on a spectrum analyzer (this is usually unnecessary). This is often a problem in setups used for verifying the performance of the noise canceller itself; the acoustic delays in acousto-optic modulators make them unsuitable for high-frequency measurements at high cancellation efficiencies, and some Pockels cells exhibit enough retardation variation across their apertures to limit attainable cancellation to 30 dB or less.

Because of the high premium placed on preserving the correlations between beams, the cancellation per-

formance tends to degrade as the optical system becomes more complicated. Étalon fringes from incidental reflections (e.g., off the windows of metal-can photodiodes) are pervasive unless great care is taken. Particularly in tuned laser experiments, such as current-tuned diode laser spectroscopy, étalon fringes cause the spectra of the two beams to differ slightly and to change rapidly with scanning, vibration, and temperature. It is noted above that a seemingly innocent antireflection-coated photodiode window can cause measurement errors of 1 part in $10^3/^\circ\text{C}$ and 3.8% per wave number due to étalon fringes alone. Errors introduced ahead of the beam sampler, which should seemingly be common mode (and hence canceled well) may sometimes not be, owing to the spatial sensitivity variations. Fringes often have a pronounced spatial structure, so they should be attended to even at points before the beam sampler.

Some optical components are worse than others; for the highest precision ratiometric measurements, components requiring near-normal incidence on one or more faces are disastrous. Cube beam splitters are particularly bad in this regard and should be replaced by Wollaston prisms or noncubical Brewster devices wherever possible. Wollaston prisms have plane-parallel faces, but because they deflect both the extraordinary and ordinary rays passing through them by an angle of $\pm 5^\circ$ to $\pm 10^\circ$, a beam entering near-normal incidence leaves the prism at a large enough angle that back reflections are much less troublesome.

Photodiode windows can be removed conveniently and safely by holding the device in a vise and gently tapping the window with a curved blunt object, such as a ball-peen hammer or a pair of gas pliers. The glass is reduced to powder, which does not damage the diode itself and is easily removed. The size of the hole in the metal case, together with the large radius of curvature of the peen, ensures that the hammer does not hit the die. The competing technique of cutting the metal can with a lathe results in oil contamination and metal slivers, which can cause short circuits. Not all photodiodes are sufficiently well passivated to perform well after long exposure to ambient conditions, so well-passivated devices should be selected. The Hamamatsu diodes used in most of the circuits for the present paper exhibited large $1/f$ noise after approximately one day of exposure to ambient conditions after their windows were removed and so appear to be poor candidates for windowless operation.

Because of the coherent addition of the incidental reflections with the main beams, the intensity perturbations caused by weak interfering beams can be surprisingly strong; $1\ \mu\text{W}$ of stray surface reflection can cause a $\pm 6.4\%$ intensity change in a 1-mW beam. Because étalon fringes are frequency dependent, they can also convert phase noise to amplitude noise, especially in multiple-longitudinal mode lasers and those (such as diode lasers) that exhibit mode hopping. The mode-hopping or mode-partition noise on the two detectors is partially decorrelated by the fringes because the relative amplitudes of the modes are changed. This extra amplitude noise will in gen-

eral be different in the two beams and so will not cancel. Because of their relatively narrow line widths, fixed-tuned single-longitudinal mode lasers should be immune to this extra noise in most cases, but it may be a limiting factor with multiple-longitudinal mode units.

Besides respecting the integrity of the laser beams, there are other constraints on the optical system. Phase shifts that are due to path delays may be important at high modulation frequencies. When a perfect canceller operation is assumed, the lower limit on modulation feedthrough for a given path-length difference Δz is

$$A_{\min} = 2 \sin\left(\frac{\pi \Delta z f_{\text{mod}}}{c}\right). \quad (16)$$

For example, if 40-dB cancellation is desired at 1-MHz modulation frequency, the path-length difference between the comparison and signal beams must be less than 0.01 rad at 1 MHz, or 48 cm. This limitation does not preclude the use of the noise canceller in long path-difference interferometers such as coherent lidars, provided that the (undelayed) local oscillator beam is significantly stronger than the delayed signal beam; in that case the delayed noise is not too large a fraction of the total noise and cancellation is effective.

Noise cancellers are quite tolerant of normal room light, but strong stray light and leaky photodiodes (such as large-area, room-temperature germanium units or longer wavelength devices with low shunt resistances, such as InAs diodes) are to be avoided, especially if the highest logarithmic output accuracy is required. Less leaky infrared photodiodes should work well, provided they can be used with at least half a volt or so of reverse bias to allow normal operation of the differential pair. PIN photodiodes should be used when possible, as they have lower capacitance for a given area. Excessive photodiode capacitance may cause the differential pair or the cascode transistor to oscillate, which will lead to poor results. Even without actual instability, capacitance will certainly degrade the high-frequency performance of the device, so when high-frequency operation is important, the smallest photodiodes that are sufficiently linear for the required current density should be used.

Because of the high SNR's they can achieve, noise cancelers are somewhat susceptible to pickup, capacitive loading on the summing junction or photodiodes, and power supply noise. They should be constructed with robust grounds (a ground-plane PC board is best, provided that the stray capacitance it adds to the summing junction of A_1 is not too large) and housed in a metal box, with the light entering through holes to aid in reducing pickup. Adequate supply by-pass capacitors (e.g., $10\text{-}\mu\text{F}$ solid tantalum in parallel with $0.1\text{-}\mu\text{F}$ monolithic ceramic from each supply to ground, on the board) and a quiet linear power supply should be used to prevent interfering signals from entering on the dc supplies. If switch-

ing supplies cannot be avoided, they should be further regulated on the card, with the use of linear voltage regulators or capacitance multipliers. The photodiodes should be mounted on the circuit board, close to transistors Q_1 – Q_3 ; they should not be put on cables, lest the cable reflections, time delays, and capacitance reduce the cancellation or destabilize the circuit. Any of these rules may of course be broken by someone sufficiently familiar with noise cancellation and low-noise design in general, but experimenters attempting to reproduce the present results in their own systems for the first few times should observe them faithfully if they desire good performance.

5. Applications and Discussion

The laser noise canceller is really a family of devices for reducing or eliminating the effects of laser amplitude noise. It operates by applying feedback outside the signal path to adjust the ratio of two photocurrents with a bipolar transistor differential pair, so that when the two are subtracted, the dc component of the result is zero. Because of the near-ideal linearity and wide bandwidth of most optical systems, photodiodes, and transistors, cancellation of the dc implies cancellation of the correlated part of the noise fluctuations as well at all frequencies of interest.

The actual noise reduction achieved by the cancellers varies from 55 dB (in the basic version) to 70 dB or more (in the high spurious suppression and differential versions). These numbers reflect the realistic behavior of the canceller in unattended technological applications, and can be improved significantly by the continual adjustment that is possible in a laboratory setting. The cancellation degrades with increasing frequency but remains useful to several megahertz, and work is going on to extend this to 100 MHz or so. The system noise floor is improved to 3 dB above the shot noise of the signal beam in the basic version and even closer with the low-noise floor and differential versions, even with noisy lasers. This is accomplished in a single operation, using a small circuit card containing approximately \$10 worth of commonly available parts.

As an added benefit, the noise canceller provides a second output related to the log ratio of the two photocurrents. The log ratio output has the same high suppression of the additive noise as the linear output and in addition has noise intermodulation suppression superior to any other technique.

The basic version of the noise canceller is limited to a dynamic range of approximately 150 dB in 1 Hz by the Johnson noise of the base spreading resistance of the bipolar transistors that are used. In applications where this is insufficient, the high-power differential version can be used to achieve 1-Hz dynamic ranges of 160 dB or higher (limited essentially by the photodiodes), equivalent to an uncertainty of 7 parts in 10^9 in 1 s.

The variations presented here are flexible enough to cover most laser-based optical measurements, and have performance good enough to replace more complicated schemes for ultrasensitive measurements

(such as heterodyne interferometry) in many cases. They are sufficiently simple, robust, and cheap to be used in real-world instruments, so that ultrasensitive measurements can be brought to cost-sensitive applications such as in-line sensors and environmental monitors. For those applications in which even more noise suppression is required, the noise cancellers can be combined with other techniques to reduce laser intensity noise, such as feedback stabilization.

Because the canceller reduces the excess noise by such a large factor, there are some subtle pitfalls in its use; these arise from a variety of seldom-noticed second-order effects. The most important of these effects are the dependence of the noise on polarization and position in the beam, photodiode nonuniformity, incidental étalon fringes, and the limitations of the bipolar transistors used in the device. The optical effects can be minimized by using a polarizer at the laser and eliminating vignetting and on-axis planar surfaces; the electronic ones by careful device selection or the use of one or more of the circuit variations presented here.

The caveats listed are not specific to this device; such problems will beset any feedback stabilization or all-electronic noise reduction system. They are more important here than elsewhere only because of the high degree of noise reduction attainable with the laser noise canceller.

Appendix A: Mathematical Results

A. Nonlinearity due to r_E

Here we derive Eq. (12) for the noise feedthrough due to r_E . Adding the effects of the degenerative feedback of the emitter bulk resistances into Eq. (3) yields

$$\frac{i_{C2}}{i_{C1}} = \exp\left(\frac{q\Delta V_{BE}}{kT}\right) \exp\left[\frac{q}{kT}(i_{C1}r_{E1} - i_{C2}r_{E2})\right]. \quad (\text{A1})$$

Assuming $ei_C r_E/kT \ll 1$, the second exponential may be replaced by the first two terms in its Maclaurin series. Differentiating implicitly and assuming that $i_{C1} + i_{C2} = i_{\text{comp}}$ and $i_{C2} = i_{\text{signal}}$ (i.e., that the current gain is infinite and the loop is in perfect balance), we obtain the partial derivatives to plug into Eq. (11), and we arrive at

$$A_{\text{min}} \approx \frac{q}{kT} \frac{(i_{\text{comp}} - i_{\text{signal}})}{i_{\text{comp}}} [r_{E1}(i_{\text{comp}} - i_{\text{signal}}) - r_{E2}i_{\text{signal}}]. \quad (\text{A2})$$

B. Shot Noise of i_{C2}

In this subsection, we derive an expression for the noise of the collector currents of a differential pair, perhaps with diode degeneration, which is fed by an emitter current source with full shot noise. If no diode degeneration is used, the collector currents have full shot noise also, regardless of the splitting ratio. We begin by introducing a simplified noise model of a BJT differential pair, which is as shown in Fig. 22; it contains only the emitter current shot-noise contribution. There are two terms in the col-

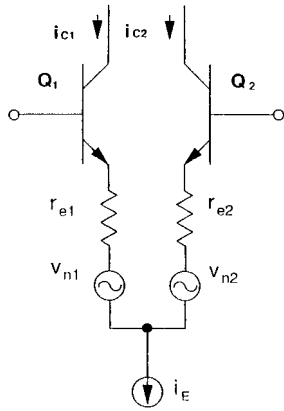


Fig. 22. Simplified noise model of a differential BJT pair.

lector noise current of Q_2 : the split emitter current noise, which splits proportionally to the emitter conductances of the transistors; and the noise current owing to the shot-noise voltages on the emitters, in series with the two emitter resistances r_e (r_e is the small-signal emitter resistance, equal to the reciprocal of the transconductance and is not the same as the emitter bulk resistance r_E). Thus the total instantaneous noise current at the collector of Q_2 is

$$i_{N2} = \frac{v_{N1} + v_{N2}}{r_{e1} + r_{e2}} + i_{NE} \left(\frac{1/r_{e2}}{1/r_{e1} + 1/r_{e2}} \right), \quad (\text{A3})$$

where

$$\langle v_N \rangle^2 = (2 qi_C) r_e^2 = \frac{2 k^2 T^2}{qi_C} \quad (\text{A4})$$

in 1-Hz bandwidth. Assuming that the current gain is high (this assumption is really in the model already) and that the three noise contributions are uncorrelated, they combine to yield

$$\langle i_{n2} \rangle^2 = 2 qi_{C2} \quad (\text{A5})$$

exactly full shot noise.

If there are N ideal diodes (such as diode-connected transistors) in series with each emitter, the values of r_e increase by a factor of $1 + N$ and the shot-noise voltages by $(1 + N)^{1/2}$. Putting these factors in, we obtain for the collector current noise

$$\langle i_{n2} \rangle^2 = 2 qi_{C2} \left(1 - \frac{N}{N + 1} \frac{i_{C1}}{i_{C1} + i_{C2}} \right). \quad (\text{A6})$$

References

1. R. L. Forward, "Wideband laser-interferometer gravitational radiation experiment," *Phys. Rev. D* **17** (2), 379–390 (1978).
2. G. R. Janik, C. B. Carlisle, and T. F. Gallagher, "Two-tone frequency-modulation spectroscopy," *J. Opt. Soc. Am. B* **3**, 1070–1074 (1986).
3. G. C. Bjorklund, "Frequency-modulated spectroscopy: a new method for measuring weak absorptions and dispersions," *Opt. Lett.* **5**, 15–17 (1980).
4. T. H. Wilmshurst, *Signal Recovery from Noise in Electronic Instrumentation* (Hilger, Boston, 1985).

5. M. A. Newkirk and K. J. Vahala, "Amplitude-phase decorrelation: a method for reducing intensity noise in semiconductor lasers," *IEEE J. Quantum Electron.* **27**, 13–22 (1991).
6. P. J. Miller, "Methods and applications for intensity stabilization of pulsed and cw lasers from 257 nm to 10.6 microns," in *Laser Noise*, R. Roy, ed., Proc. SPIE **1376**, 180–191 (1991).
7. E. Ingelstam, "Some quantitative measurements of path differences and gradients by means of phase contrast and new interferometric devices," *J. Opt. Soc. Am.* **47**, 536–544 (1957).
8. R. Stierlin, R. Bättig, P.-D. Henchoz, and H. P. Weber, "Excess noise suppression in a fibre-optic balanced heterodyne detection system," *Opt. Quantum Electron.* **18**, 445–454 (1986).
9. R. P. Moeller and W. K. Burns, "1.06 μm all-fiber gyroscope with noise subtraction," *Opt. Lett.* **16**, 1902–1904 (1991).
10. B. Wandernoth, "20 photon/bit 565 Mbit/s PSK homodyne receiver using synchronization bits," *Electron. Lett.* **28** (4), 387–388 (1992).
11. C. J. Peters, "Laser communications system employing narrow band noise cancellation," U.S. patent 3,465,156 (2 Sept. 1969).
12. P. C. D. Hobbs, "Reaching the shot noise limit for \$10," *Opt. Photon. News* **2** (4), 17–23 (1991).
13. P. C. D. Hobbs, "Shot noise limited optical measurements at baseband with noisy lasers," in *Laser Noise*, R. Roy, ed., Proc. SPIE **1376**, 216–221 (1991).
14. P. C. D. Hobbs, "Noise cancelling circuitry for optical systems, with signal dividing and combining means," U.S. patent 5,134,276 (28 July 1992).
15. K. L. Haller and P. C. D. Hobbs, "Double beam laser absorption spectroscopy: shot-noise limited performance at baseband with a novel electronic noise canceller," in *Optical Methods for Ultrasensitive Detection and Analysis: Techniques and Applications*, B. L. Fearey, ed., Proc. SPIE **1435**, 298–309 (1991).
16. C. L. A. Collins, K. D. Bonin, and M. A. Kadar Kallen, "Absolute two photon cross section of Rb measured by differential absorption," *Opt. Lett.* **18**, 1754–1756 (1993).
17. P. C. D. Hobbs, "ISICL: *in situ* coherent lidar for particle detection in semiconductor processing equipment," *Appl. Opt.* **34**, 1579–1590 (1995).
18. M. D. Levenson, W. H. Richardson, and S. H. Perlmuter, "Stochastic noise in TEM₀₀ laser-beam position," *Opt. Lett.* **14**, 779–781 (1989).
19. D. L. Heinz, J. S. Sweeney, and P. Miller, "A laser heating system that stabilizes and controls the temperature: diamond anvil cell applications," *Rev. Sci. Instrum.* **62**, 1568–1575 (1991).
20. M. C. Nuss, U. H. Keller, G. T. Harvey, M. S. Heutmaker, and P. R. Smith, "Amplitude noise reduction of 50 dB in colliding-pulse mode-locking dye lasers," *Opt. Lett.* **15**, 1026–1028 (1990).
21. Yu. N. Dubnitshev, V. P. Koronkevich, V. S. Sobolev, A. A. Stolpovski, Yu. G. Vasilenko, and E. N. Utkin, "Laser Doppler velocimeter as an optoelectronic data processing system," *Appl. Opt.* **14** (1), 180–184 (1975).
22. B. Reuter and N. Talukder, "A new differential laser microanemometer," in *1980 European Conference on Optical Systems and Applications*, D. J. Kroon, ed., Proc. SPIE **236**, 226–230 (1980).
23. S. Okamura and M. Maruyama, "Improvement on the sensitivity of electro-optical system for electric field strength measurements," *Trans. Inst. Electron. Commun. Eng. Jpn. E* **65**, 702 (1982).
24. National Semiconductor, Inc., "LM13600 data sheet," in *Operational Amplifiers Data Book* (National Semiconductor, Santa Clara, Calif., 1990).
25. Precision Monolithics, Inc., PM-1008 data sheet, in *Analog IC Data Book* (Precision Monolithics, Inc., Santa Clara, Calif., 1990), Vol. 10, pp. 5-556 to 5-566.